Infrared Physics & Technology 53 (2010) 419–424

Contents lists available at ScienceDirect

Infrared Physics & Technology

journal homepage: www.elsevier.com/locate/infrared

Regular article

Numerical optimization of an ambient temperature photoelectromagnetic detector for middle and far infrared spectral regions

R. Hazrati [a], S. Shojaei [b,*], M. Karimi [c], M. Kalafi [b]

[a] Physics Department, University of Tabriz, Tabriz, Iran
[b] Research Institute for Applied Physics and Astronomy, Photonics–Electronics Group, University of Tabriz, P.O. Box 51665-163, Tabriz, Iran
[c] Department of Physics, Azerbaijan University of Tarbiat Moallem, Tabriz, Iran

ARTICLE INFO

Article history:
Received 8 April 2010
Available online 3 August 2010

Keywords:
Photoelectromagnetic effect
Infrared detector
Responsivity
Specific detectivity
Response time
MCT

ABSTRACT

The specific detectivity of p-type PEM detectors based on $Hg_{1-x}Cd_xTe$ (MCT), has been optimized for 10.6 μm and 4 μm wavelengths in atmospheric windows. A system of transport equations with Poisson equation, have been solved self consistently in the presence of external magnetic field. The values of responsivity (R_v), specific detectivity (D^*) and response time (τ_r) have been analyzed in achieved optimum condition. Our results show that the specific detectivity and responsivity of PEM detector in the middle infrared region is at least one order of magnitude greater than those in far infrared. In contrast, the response time in far infrared region is very short. The obtained optimized values of detectivity in 10.6 μm and 4 μm are 3.59×10^7 cm $Hz^{\frac{1}{2}}$ W^{-1} and 3.75×10^8 cm $Hz^{\frac{1}{2}}$ W^{-1}, respectively. These results are in reasonable agreement with experimental results.

1. Introduction

Cooling is a considerable problem which inhibits the more widespread application of infrared technology. In fact it is a direct, straightforward and the most efficient way to suppress the thermal generation. At the same time cooling is a very impractical method. So it is clear that operation of a typical detector without cooling is most useful because they could be light weight, rugged, reliable and convenient to use. Affordable high performance infrared systems require cost-effective infrared detectors that operate without cooling [1–12]. Thus special attention is put on realization and optimization of the devices for room temperature operation having short response time [4,8,12,13]. Recently uncooled operation of IR detectors has been reported [1–4,13–15]. The photoelectromagnetic (PEM) effect has been traditionary used for ambient temperature photoconductors in the middle and far infrared band. Advantages of the PEM detector are short response time, lack of the bias that causes low level of noise and low resistance enabling the use of fast electronic [3,4,9,15,17,18]. Also, it was shown that cooling of PEM detectors are rather rarely used [3,10]. A promising material for the construction of photodetectors is Mercury Cadmium Telluride ($Hg_{1-x}Cd_xTe$) which enables tuning wavelength over a wide spectrum range. $Hg_{1-x}Cd_xTe$ exhibits extreme flexibility, it can be tailored for optimized detection at any region of the IR spectrum. Also among various variable band gap semiconductor alloys, $Hg_{1-x}Cd_xTe$ is the only material covering the whole IR spectral range. MCT can be used for detection in 3–5 μm and 8–12 μm atmospheric windows which has also attracted some interest due to maximum transparency of IR wavelengths in these spectral regions [3–6,8,12–15,19–37].

In this paper, we have optimized the specific detectivity of uncooled PEM detectors based on MCT for 10.6 μm (CO_2 laser wavelength) and 4 μm in atmospheric windows. For this purpose, we numerically solved the equations of transport of carriers with Poisson's equation in the presence of external magnetic field in a self-consistent way. Also we have determined responsivity and response time in the optimum condition. Finally we compared obtained results for two above mentioned spectral regions.

2. Theoretical considerations

The PEM effect is caused by an in-depth diffusion of photogenerated carriers whose trajectories are deflected in a magnetic field. The deriving force for diffusion is the gradient of carrier concentration that is caused by the non-uniform absorption of radiation in the different layers of bulk semiconductor.

The current components in the semiconductor in the presence of a magnetic and electric field and a concentration gradient can be written as [38]:

$$J_{hx} = qp\mu_h E_x + \mu_h B J_{hy} \quad (1)$$

* Corresponding author. Tel.: +98 4113393006; fax: +98 4113347050.
E-mail addresses: s_shojaei@tabrizu.ac.ir, shojaei.sh@gmail.com (S. Shojaei).

1350-4495/$ - see front matter © 2010 Elsevier B.V. All rights reserved.
doi:10.1016/j.infrared.2010.07.009

$$J_{hy} = qp\mu_h E_y - \mu_h B J_{hx} - qD_h \frac{\partial p}{\partial y} \tag{2}$$

$$J_{ex} = qn\mu_e E_x - \mu_e B J_{ey} \tag{3}$$

$$J_{ey} = qn\mu_e E_y + \mu_e B J_{ex} + qD_e \frac{\partial n}{\partial y} \tag{4}$$

where J_e and J_h are electron and hole current densities, respectively, n and p are electron and hole concentrations, μ_e and μ_h are the carrier mobilities, D_e and D_h are the diffusion coefficients, q is the magnitude of the elementary electric charge, B is the magnetic field (in the z direction) and E_x and E_y are the x and y components of the electric field. Assuming continuity condition of current over the surface and the entire volume, one can define electron and hole current densities in y direction as $J = J_{ey} = -J_{hy}$. There are three important carrier recombination mechanisms in HgCdTe: Shockley–Read-Hall (SRH), radiative, and Auger recombination. In SRH mechanism, recombination occurs via lattice defect and impurity energy levels within the forbidden energy gap of semiconductor. In principle, it may be reduced by lowering concentrations of native defects and foreign impurities. Thus the Shockley–Read-Hall mechanism does not represent the fundamental limit to performance of room temperature photodetectors being prepared from the narrow band gap semiconductors like MCT. From Fig. 1, It can be seen that Auger 1 recombination time is increasing and Auger 7 recombination time is rapidly decreasing with increasing acceptor concentration and consequently increasing hole concentration and decreasing electron concentration. From Fig. 2, it is clear that by increasing the acceptor dopping level slowly, Auger time is increasing slowly because, the Auger 1 increases and reaches its maximum value and then it decreases due to rapid decreasing of Auger 7, as also shown in Fig. 1.

We define Auger time and effective time as:

$$\frac{1}{\tau_A} = \frac{1}{\tau_{A1}} + \frac{1}{\tau_{A7}} \tag{5}$$

$$\frac{1}{\tau_{eff}} = \frac{1}{\tau_A} + \frac{1}{\tau_{RAD}} \tag{6}$$

From Fig. 2, it is clear that due to coincidence of the effective time values on Auger time values, the dominant recombination mechanism is Auger process.

Thus the continuity equation may be written as:

$$\frac{\partial J}{\partial y} = qU = q(R_{A1} + R_{A7} - G_{opt}) \tag{7}$$

where U is the net recombination rate and R_{A1} and R_{A7} denotes Augers 1 and 7 recombination rates, respectively and G_{opt} denotes optical generation rate. Here we have assumed that the optical generation rate of excess carriers varies exponentially with increasing depth, namely:

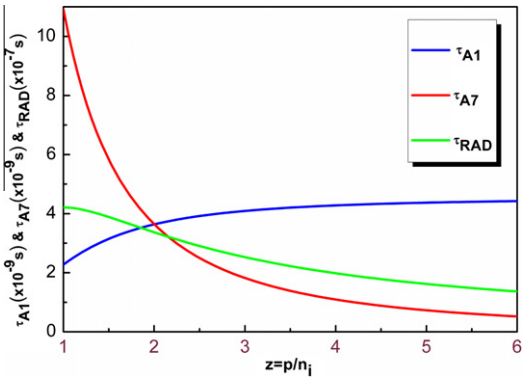

Fig. 1. Augers 1 and 7 and radiative times versus dopping in the room temperature.

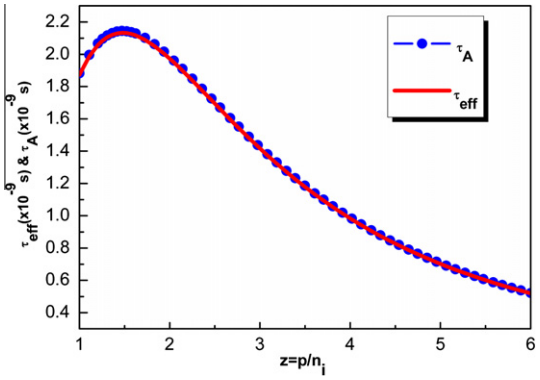

Fig. 2. Effective and Auger times versus dopping in the room temperature.

$$G_{opt} = \alpha\eta\Phi(1 - R_1)e^{-\alpha y} \tag{8}$$

where α is the absorption coefficient, η is the quantum efficiency, Φ is the photon flux density on the sample and R_1 is the reflectivity of the near (illuminated) surface of semiconductor.

By the combination of Eqs. (1)–(4), (and) (7) we obtain below equations for p, n and J:

$$D_h \frac{\partial^2 p}{\partial y^2} + (\mu_h^2 B E_x - \mu_h E_y)\frac{\partial p}{\partial y} - \mu_h \frac{\partial E_y}{\partial y} p - \left(1 + \mu_h^2 B^2\right) U = 0 \tag{9}$$

$$D_e \frac{\partial^2 n}{\partial y^2} + (\mu_e^2 B E_x + \mu_e E_y)\frac{\partial n}{\partial y} + \mu_e \frac{\partial E_y}{\partial y} n - \left(1 + \mu_e^2 B^2\right) U = 0 \tag{10}$$

$$J = \frac{k_B T \mu_e \mu_h \left(p\frac{\partial n}{\partial y} + n\frac{\partial p}{\partial y}\right) + qnp\mu_e\mu_h(\mu_e + \mu_h)BE_x}{n\mu_e\left(1 + \mu_h^2 B^2\right) + p\mu_h\left(1 + \mu_e^2 B^2\right)} \tag{11}$$

where k_B is the Boltzmann's constant and T is absolute temperature. The boundary condition at a surface is specified in terms of an effective surface recombination velocity S through an equation of the form:

$$J|_{surface} = qS\left(\frac{np - n_0 p_0}{n_0 + p_0}\right)\Big|_{surface} \tag{12}$$

n_0 and p_0 are the thermal equilibrium electron and hole concentrations [38]. In addition Eqs. (1)–(4) must still be satisfied in boundaries also, thus the boundary condition to solve Eqs. (9) and (10) are, respectively:

$$p(0)\mu_h E_y(0) - p(0)\mu_h^2 B E_x - D_h \frac{\partial p(0)}{\partial y} + \left(1 + \mu_h^2 B^2\right) S_1 \left(\frac{n(0)p(0) - n_0 p_0}{n_0 + p_0}\right) = 0 \tag{13}$$

$$p(d)\mu_h E_y(d) - p(d)\mu_h^2 B E_x - D_h \frac{\partial p(d)}{\partial y} - (1 + \mu_h^2 B^2) S_2 \left(\frac{n(d)p(d) - n_0 p_0}{n_0 + p_0}\right) = 0 \tag{14}$$

$$n(0)\mu_e E_y(0) + n(0)\mu_e^2 B E_x + D_e \frac{\partial n(0)}{\partial y} - (1 + \mu_e^2 B^2) S_1 \left(\frac{n(0)p(0) - n_0 p_0}{n_0 + p_0}\right) = 0 \tag{15}$$